# *Contents*

**S1.** The UHPLC-HRMS$^2$ analysis
**S2.** Source apportionment using Positive Matrix Factorization (PMF)
**S3.** Calculations of ALWC, aerosol pH with thermodynamic modeling
**Table S1.** Details of collected samples.
**Table S2.** The monitoring instruments in different sites.
**Table S3.** CD workflow
**Table S4.** Overview of detected OS and NOS compounds in this work that were also identified in previous studies.
**Table S5** The formula, classification, and MS$^2$ fragments of Unknown OSs and NOSs
**Table S6.** The mass concentrations of $PM_{2.5}$ and its chemical composition, gaseous pollutants concentrations, and the mean values of the meteorological parameters.
**Figure S1.** The geographical locations of the sample sites in this study.
**Figure S2.** Time series of Ba, K, Fe and Mn concentrations in Changsha.
**Figure S3.** Time series of chemical components concentrations in Changsha.
**Figure S4.** Contribution of different sources to $PM_{2.5}$ mass in three sites.
**Figure S5.** Aerosol liquid water content (ALWC) as a function of the relative humidity (RH).
**Figure S6.** The mass concentrations of OSs under different pH levels.
**Figure S7.** Diurnal variations of the distribution of $NO_2$, and $O_3$ on $O_x$ in (a) Changsha, (b) Taiyuan, and (c) Beijing.

## S1. The UHPLC-HRMS$^2$ analysis

The UHPLC-HRMS system was used for sample extraction analysis with full scan and higher-energy collisional dissociation (HCD). Chromatographic separation was performed on a reversed-phase column (Accucore C18, 150×2.1 mm, 2.6 μm particle size, Thermo Scientific) with a flow rate of 0.33 mL/min and an injection volume of 2.5 μL. Mobile phase A consisted of ultrapure water with 0.05% acetic acid, while mobile phase B was a mixture of methanol and 0.05% acetic acid. The HPLC gradient program was as follows: from 0 to 1.5 minutes, the composition was held at 5% B; then, from 1.5 to 8 minutes, it linearly increased to 54% B; subsequently, from 8 to 11 minutes, it linearly changed to 95% B; next, from 11 to 12 minutes, it linearly reached 100% B, holding for 2 minutes, and then, from 14 to 14.5 minutes, it linearly returned to 5% B with a 1.5 minutes hold before the next injection. The settings were as follows: capillary voltage -3.5 kV, capillary temperature 320 ℃, vaporizer temperature 35 ℃, and sheath, auxiliary, and sweep gas at 2, 1, and 1 arbitrary unit, respectively.

The HRMS operated in negative ESI mode, employing data-dependent acquisition (DDA). Full scan (MS1, $m/z$ = 70–700, resolving power 120000) and fragmentation scan (MS2) for the top ten ions ($m/z$ = 50–500, resolving power 30,000, collision energies 30, 40, and 50 eV, intensity threshold 50000) were collected. The HRMS peaks with more than 2 charges were excluded. The other settings were kept the same as in the full scan mode. An instrumental blank (methanol) was injected every 10 samples to monitor any instrumental background.

## S2. Source apportionment using Positive Matrix Factorization (PMF)

USEPA-PMF 5.0 software was performed on $PM_{2.5}$ for the entire sampling period. The input data for the PMF consists of a concentration matrix and an uncertainty matrix for chemically speciated concentrations of components of $PM_{2.5}$ (carbonaceous fractions, WSIIs or the water-soluble inorganic species, and trace elements), where the rows correspond to the time series, and the columns to the species.

The chemical species included were carbonaceous fractions namely organic carbon, and elemental carbon (EC); water-soluble inorganic species namely $SO_4^{2-}$, $NO_3^-$, $Cl^-$, $NH_4^+$, $K^+$, $Ca^{2+}$, $Na^+$, $K^+$; trace elements namely Al, Si, Ti, Cr, Mn, Fe, Se, Co, Ni, Cu, Zn, As, Br, Sr, Pb, V and K. Species with a S/N ratio > 1 were designated as strong, while S/N ratios < 0.5 were designated as bad. The best solution for the base run was obtained using seven factors: biomass burning, fireworks and crackers, coal combustion, traffic emissions, road dust, secondary inorganics, industry combustion.

## S3. Calculations of ALWC, aerosol pH with thermodynamic modeling

The aerosol liquid water content (ALWC) was calculated using the ISORROPIA II thermodynamic model. The model input data mainly include the mass concentration of water-soluble ions (chloride, sulfate, nitrate, and ammonium, in μg/m$^3$), temperature (in Kelvin), and ambient RH (ranging from 0 to 1). We employed ISORROPIA-II in "forward" mode, and he model assumes aerosol was in a "metastable" state with internally mixed and in thermodynamic equilibrium with the gas phase. The calculated ALWC was lower than the actual ALWC because the aerosol liquid water associated with water-soluble organic species was not included (Fountoukis and Nenes, 2007). The pH was calculated by the using eq.(S1):

$$pH = -\log_{10}\frac{1000H^{+}_{air}}{ALWC} \quad (S1)$$

where $H_{air}^{+}$ is $H^{+}$ loading per volume air (μg/m$^3$).

**Table S1.** Details of collected samples.

| Sampling ID* | Sampling period | Average $PM_{2.5}$ (μg/m$^3$) | Average RH (%) |
|---|---|---|---|
| TY1211H | 23.0 h | 114.63 | 79.61 |
| TY1212H | 23.0 h | 59.89 | 79.88 |
| TY1213H | 23.0 h | 32.83 | 79.25 |
| TY1214H | 15.0 h | 22.63 | 91.07 |
| TY1214M | 8.0 h | 17.59 | 57.99 |
| TY1217M | 23.0 h | 46.82 | 45.81 |
| TY1218H | 6.8 h | 193.38 | 71.49 |
| TY1218L | 6.8 h | 35.74 | 30.34 |
| TY1218M | 9.4 h | 168.33 | 45.95 |
| TY1220L | 23.0 h | 10.58 | 31.34 |
| TY1221L | 9.2 h | 39.87 | 30.64 |
| TY1221M | 13.8 h | 28.70 | 47.44 |
| TY1222H | 6.6 h | 70.07 | 62.81 |
| TY1222L | 6.5 h | 86.49 | 36.99 |
| TY1222M | 9.9 h | 95.72 | 50.06 |
| TY1223L | 9.5 h | 40.97 | 37.64 |
| TY1223M | 13.5 h | 40.46 | 55.08 |
| TY1224H | 3.5 h | 60.89 | 62.27 |
| TY1224L | 6.5 h | 64.85 | 33.91 |
| TY1224M | 13.0 h | 66.47 | 52.43 |
| TY1225H | 9.0 h | 54.50 | 64.82 |
| TY1225L | 8.0 h | 48.57 | 31.30 |
| TY1225M | 6.0 h | 84.01 | 52.48 |
| TY1226H | 4.5 h | 64.47 | 65.85 |
| TY1226L | 6.4 h | 82.40 | 33.37 |
| TY1226M | 12.1 h | 48.49 | 50.49 |
| TY1227H | 10.5 h | 102.23 | 70.51 |
| TY1227L | 3.8 h | 80.45 | 36.76 |
| TY1227M | 8.7 h | 101.14 | 51.31 |
| TY1228H | 13.9 h | 137.82 | 70.13 |
| TY1228L | 3.4 h | 97.64 | 35.22 |
| TY1228M | 5.7 h | 155.63 | 48.82 |
| TY1229H | 16.6 h | 246.03 | 76.81 |
| TY1229M | 6.4 h | 247.11 | 56.38 |
| TY1230H | 23.0 h | 34.05 | 67.95 |
| TY1231M | 16.4 h | 74.79 | 59.05 |
| TY1231L | 6.6 h | 20.37 | 36.19 |
| TY0101H | 13.6 h | 133.94 | 71.40 |
| TY0101M | 9.4 h | 138.30 | 51.48 |
| TY0102L | 8.7 h | 23.80 | 32.56 |
| TY0102M | 14.3 h | 24.69 | 53.91 |
| TY0103H | 6.0 h | 45.26 | 61.92 |

67 **Table S1** Continued

| Sampling ID* | Sampling period | Average $PM_{2.5}$ (μg/m$^3$) | Average RH (%) |
|---|---|---|---|
| TY0103L | 8.4 h | 39.07 | 32.81 |
| TY0103M | 8.6 h | 60.97 | 54.97 |
| TY0104L | 15.1 h | 38.52 | 30.19 |
| TY0104M | 7.9 h | 29.48 | 48.30 |
| TY0106L | 16.2 h | 16.22 | 29.59 |
| TY0106M | 6.8 h | 17.94 | 43.27 |
| TY0107L | 8.7 h | 36.26 | 22.63 |
| TY0107M | 14.3 h | 47.55 | 48.34 |
| TY0108H | 14.3 h | 109.21 | 61.37 |
| TY0108L | 6.2 h | 103.28 | 34.61 |
| TY0108M | 2.5 h | 76.61 | 49.75 |
| TY0109H | 7.8 h | 44.57 | 65.18 |
| TY0109L | 3.5 h | 48.94 | 38.17 |
| TY0109M | 11.7 h | 49.84 | 48.90 |
| TY0110H | 8.3 h | 70.48 | 66.80 |
| TY0110L | 5.1 h | 64.41 | 38.37 |
| TY0110M | 9.6 h | 69.07 | 44.51 |
| TY0111H | 5.9 h | 95.34 | 63.55 |
| TY0111L | 6.9 h | 81.94 | 34.07 |
| TY0111M | 10.2 | 89.66 | 53.17 |
| TY0113L | 8.9 h | 81.32 | 32.63 |
| TY0113M | 14.1 h | 68.30 | 45.10 |
| BJ1203L | 13.0 h | 41.97 | 26.06 |
| BJ1203M | 10.0 h | 52.61 | 45.80 |
| BJ1208L | 6.0 h | 90.98 | 23.39 |
| BJ1208M | 17.0 h | 59.02 | 42.40 |
| BJ1209L | 3.2 h | 36.43 | 27.27 |
| BJ1209M | 19.8 h | 28.11 | 43.65 |
| BJ1210L | 5.5 h | 31.61 | 37.28 |
| BJ1210H | 17.5 h | 24.17 | 82.23 |
| BJ1211H | 23.0 h | 28.44 | 82.41 |
| BJ1212H | 23.0 h | 59.76 | 85.39 |
| BJ1213H | 23.0 h | 82.85 | 84.82 |
| BJ1215L | 23.0 h | 6.15 | 33.01 |
| BJ1216L | 23.0 h | 7.65 | 28.00 |
| BJ1217L | 9.0 h | 16.99 | 27.52 |
| BJ1217M | 14.0 h | 30.27 | 56.72 |
| BJ1218H | 5.2 h | 79.38 | 63.45 |
| BJ1218L | 7.6 h | 33.86 | 29.21 |
| BJ1218M | 10.2 h | 74.80 | 53.15 |
| BJ1222M | 12.7 h | 29.53 | 48.35 |
| BJ1222L | 10.3 h | 19.87 | 25.09 |

**Table S1** Continued

| Sampling ID* | Sampling period | Average $PM_{2.5}$ (μg/m$^3$) | Average RH (%) |
|---|---|---|---|
| BJ1224H | 6.6 h | 35.68 | 64.80 |
| BJ1224L | 5.9 h | 30.02 | 21.95 |
| BJ1224M | 10.5 h | 35.38 | 47.11 |
| BJ1225H | 3.7 h | 79.82 | 64.16 |
| BJ1225L | 6.7 h | 36.29 | 27.30 |
| BJ1225M | 12.6 h | 58.16 | 51.90 |
| BJ1226H | 8.3 h | 24.48 | 66.41 |
| BJ1226L | 2.8 h | 20.30 | 30.58 |
| BJ1226M | 11.9 h | 25.74 | 53.09 |
| BJ1227H | 11.5 h | 31.91 | 71.11 |
| BJ1227L | 5.8 h | 24.02 | 31.57 |
| BJ1227M | 5.7 h | 25.75 | 50.03 |
| BJ1228H | 11.9 h | 57.99 | 72.07 |
| BJ1228L | 5.6 h | 50.83 | 31.71 |
| BJ1228M | 5.5 h | 52.15 | 50.38 |
| BJ1229H | 15.2 h | 155.75 | 75.91 |
| BJ1229L | 5.3 h | 67.75 | 34.60 |
| BJ1229M | 2.5 h | 93.97 | 45.40 |
| BJ1230L | 7.3 h | 19.84 | 37.22 |
| BJ1230M | 15.7 h | 105.58 | 46.27 |
| CS1211 | 23.0 h | 12.15 | 89.30 |
| CS1212 | 23.0 h | 30.34 | 78.37 |
| CS1213 | 23.0 h | 29.52 | 84.29 |
| CS1214 | 23.0 h | 32.04 | 91.23 |
| CS1215 | 23.0 h | 16.10 | 85.37 |
| CS1216 | 23.0 h | 18.67 | 53.45 |
| CS1217 | 23.0 h | 20.93 | 48.84 |
| CS1218 | 23.0 h | 27.36 | 87.01 |
| CS1219 | 23.0 h | 41.75 | 74.37 |
| CS1220 | 23.0 h | 34.38 | 76.16 |
| CS1221 | 23.0 h | 51.23 | 63.41 |
| CS1222 | 23.0 h | 31.67 | 41.99 |
| CS1223 | 23.0 h | 39.62 | 53.17 |
| CS1224 | 23.0 h | 54.91 | 57.05 |
| CS1225 | 23.0 h | 73.04 | 56.77 |
| CS1226 | 23.0 h | 60.96 | 43.26 |
| CS1227 | 23.0 h | 97.74 | 63.02 |
| CS1228 | 23.0 h | 159.01 | 73.79 |
| CS1229 | 23.0 h | 216.33 | 75.10 |
| CS1230 | 23.0 h | 180.26 | 83.05 |
| CS1231 | 23.0 h | 132.52 | 80.59 |
| CS0101 | 23.0 h | 86.49 | 67.63 |

**Table S1** Continued

| Sampling ID* | Sampling period | Average $PM_{2.5}$ (μg/m$^3$) | Average RH (%) |
|---|---|---|---|
| CS0102 | 23.0 h | 80.91 | 85.15 |
| CS0103 | 23.0 h | 45.99 | 76.24 |
| CS0104 | 23.0 h | 57.02 | 70.55 |
| CS0105 | 23.0 h | 56.16 | 71.98 |
| CS0106 | 23.0 h | 61.91 | 72.81 |
| CS0107 | 23.0 h | 82.71 | 75.75 |
| CS0108 | 23.0 h | 74.73 | 83.14 |
| CS0109 | 23.0 h | 75.18 | 80.60 |

* TY is short for Taiyuan, BJ for Beijing, and CS for Changsha. In the Beijing and Taiyuan samples, the labels H, M, and L represent high (RH > 60 %), moderate (40 % < RH ⩽ 60 %), and low (RH ⩽ 40 %) RH regimes, respectively.

**Table S2.** The monitoring instruments in different sites.

| Sample site | Instruments | Measured Parameters |
|---|---|---|
| Changsha | Ion Chromatography (IC) (DIONEX ICS2000) | water-soluble inorganic ions |
| | Gas Chromatography - Mass Spectrometry (GC-MS) (Agilent 7890B-5977A) | VOCs |
| | OC-EC aerosol analyzer (Sunset Lab Model 5L) | EC, OC |
| | Automatic gas analyzers (Thermo scientific Model 42i, 43i, 48i, 49i) | $NO_x$, $SO_2$, CO, $O_3$ |
| | X-ray Fluorescence (XRF) (Panalytical Zetium) | trace elements |
| Taiyuan | Monitor for AeRosols and Gases in ambient Air (MARGA) (Metrohm 2060) | water-soluble inorganic ions |
| | GC-MS (Shimadzu QP2010SE) | VOCs |
| | Carbon Aerosol Speciation System (CASS) (Aerosol Magee Scientific) | EC, OC |
| | Three-arm impactor (Home-made) | the particle rebound fraction |
| | Automatic gas analyzers (Thermo scientific Model 42i, 43i, 48i, 49i) | $NO_x$, $SO_2$, CO, $O_3$ |
| | XRF (Panalytical Zetium) | trace elements |
| Beijing | MARGA (Metrohm 2060) | water-soluble inorganic ions |
| | Automatic gas analyzers (Thermo scientific Model 42i, 43i, 48i, 49i) | $NO_x$, $SO_2$, CO, $O_3$ |
| | GC-MS (Shimadzu QP2010SE) | VOCs |
| | OC-EC aerosol analyzer (Sunset Lab Model 5L) | EC, OC |
| | XRF (Panalytical Zetium) | trace elements |

**Table S3.** CD workflow

| | | |
|---|---|---|
| Select Spectra | | |
| Spectrum Properties Filter Scan Event Filters | Lower RT Limit | 0 |
| | Upper RT Limit | 0 |
| | Polarity Mode | Negative |
| Align Retention Times | | |
| General Settings | Alignment Model | Adaptive curve |
| | Maximum Shift [min] | 2 |
| | Mass Tolerance | 5 ppm |
| Detect Compounds | | |
| General Settings | Mass Tolerance [ppm] | 5 ppm |
| | Min. Peak Intensity | 10000 |
| | Use Most Intense Isotope Only | True |
| Peak Detection | Chromatographic S/N Threshold | 3 |
| | Remove Baseline | False |
| Isotope Pattern Detection | Group Isotopes for | Br; Cl |
| Compound Detection | Ions | [M-H]-1; [M-H-$H_2O$]-1; [2M-H]-1 |
| Group Compounds | | |
| General Settings | Mass Tolerance | 5 ppm |
| | RT Tolerance [min] | 0.5 |
| | Align Peaks | False |
| | Preferred Ions | [M-H]-1; [M-H-$H_2O$]-1; [2M-H]-1 |
| | Area Integration | Most Common Ion |
| Peak Rating Contributions | Area Contribution | 3 |
| | CV Contribution | 10 |
| | FWHM to Base Contribution | 5 |
| | Jaggedness Contribution | 5 |
| | Modality Contribution | 5 |
| | Zig-Zag Index Contribution | 5 |
| Peak Rating Filter | Peak Rating Threshold | 0 |
| | Number of Files | 0 |
| Merge Features | | |
| Peak Consolidation | Mass Tolerance | 5 ppm |
| | RT Tolerance [min] | 0.5 |
| Search mzCloud | | |
| General Settings | Compound Classes | All |
| | Library | Autoprocessed; Reference |
| | Search MSn Tree | False |

**Table S3** Continued

| | | |
|---|---|---|
| Search mzCloud | | |
| DDA Search | Identity Search | Cosine |
| | Match Activation Type | False |
| | Match Activation Energy | Any |
| | Activation Energy Tolerance | 20 |
| | Apply Intensity Threshold | True |
| | Similarity Search | Confidence Reverse |
| | Match Factor Threshold | 30 |
| | Use DIA Scans for Search | True |
| | Max. Isolation Width [Da] | 500 |
| DIA Search | Match Activation Type | False |
| | Match Activation Energy | Any |
| | Activation Energy Tolerance | 100 |
| | Apply Intensity Threshold | True |
| | Match Factor Threshold | 20 |
| Predict Compositions | | |
| Prediction Settings | Mass Tolerance | 5 ppm |
| | Min. Element Counts | C H |
| | Max. Element Counts | C90 H200 N5 O20 S2 |
| | Min. RDBE | 0 |
| | Max. RDBE | 40 |
| | Min. H/C | 0.3 |
| | Max. H/C | 3.5 |
| | Max. # Candidates | 10 |
| Pattern Matching | Intensity Tolerance [%] | 30 |
| | Intensity Threshold [%] | 0.1 |
| | S/N Threshold | 3 |
| Fragments Matching | Use Dynamic Recalibration | True |
| | Use Fragments Matching | True |
| | Mass Tolerance | 5 ppm |
| | S/N Threshold | 3 |
| Assign Compound Annotations | | |
| General Settings Scoring Rules | Mass Tolerance | 5 ppm |
| | Use mzLogic | True |
| | Use Spectral Distance | True |
| | SFit Threshold | 20 |
| | SFit Range | 20 |
| Data Sources | Data Source #1 | mzCloud Search |
| | Data Source #2 | mzVault Search |
| | Data Source #3 | Predicted Compositions |
| | Data Source #4 | ChemSpider Search |
| Reprocessing | Clear Names | False |

81 **Table S3** Continued

| | | |
|---|---|---|
| Search ChemSpider | | |
| Search Settings | Database(s) | ACToR: Aggregated Computational Toxicology Resource; DrugBank; EAWAG Biocatalysis/Biodegradation Database; EPA DSSTox; EPA Toxcast; FDA UNII-NLM; Nature Chemistry; Sigma-Aldrich |
| | Search Mode | By Formula or Mass |
| | Mass Tolerance | 5 ppm |
| | Max. # of results per compound | 20 |
| | Max. # of Predicted Compositions to be searched per Compound | 3 |
| Fill Gaps | | |
| General Settings | Mass Tolerance | 5 ppm |
| | S/N Threshold | 1.5 |
| Mark Background Compounds | | |
| General Settings | Max. Sample/Blank | 5 |
| | Max. Blank/Sample | 0 |
| | Hide Background | True |
| Apply Spectral Distance | | |
| Pattern Matching | Mass Tolerance | 5 ppm |
| | Intensity Tolerance [%] | 30 |
| | Intensity Threshold [%] | 0.1 |
| | S/N Threshold | 3 |
| | Use Dynamic Recalibration | True |
| Apply mzLogic | | |
| Search Settings | Max. # Compounds | 0 |
| | Max. # mzCloud Similarity Results to consider per Compound | 10 |
| | Match Factor Threshold | 30 |

82

83

**Table S4.** Overview of detected OSs and NOSs compounds in this work that were also identified in previous studies.

| Formula | m/z ([M-H]$^-$) | RT (min) | Previous studies |
|---|---|---|---|
| **Aromatic OSs and NOSs** | | | |
| $C_8H_6O_5S$ | 212.98532 | 0.88 | (Yang et al., 2024) |
| $C_8H_{14}O_{10}S$ | 301.02349 | 0.99 | (Yang et al., 2024) |
| $C_9H_{12}O_5S$ | 231.03327 | 0.90 | (Riva et al., 2015) |
| $C_9H_{14}O_7S$ | 265.03875 | 1.01 | (Yang et al., 2020) |
| $C_9H_{18}O_8S$ | 285.06496 | 1.03 | (Riva et al., 2016) |
| $C_9H_{14}O_8S$ | 281.03366 | 0.99 | (Yang et al., 2020) |
| $C_{10}H_{12}O_7S$ | 275.02310 | 0.99 | (Riva et al., 2015) |
| $C_{11}H_{12}O_7S$ | 287.02310 | 1.00 | (Le Breton et al., 2018) |
| $C_{11}H_{20}O_{11}S$ | 359.06536 | 1.12 | (Yang et al., 2024) |
| $C_{10}H_{10}O_7S$ | 273.00745 | 1.01 | (Riva et al., 2015) |
| $C_{11}H_{14}O_7S$ | 289.03875 | 1.04 | (Riva et al., 2015) |
| $C_9H_{13}O_9NS$ | 310.02383 | 0.94 | (Yang et al., 2020) |
| **Aliphatic OSs** | | | |
| $C_8H_{18}O_4S$ | 209.08530 | 10.06 | (Huang et al., 2023) |
| $C_9H_{18}O_4S$ | 221.08530 | 10.62 | (Yang et al., 2024) |
| $C_9H_{18}O_5S$ | 237.08022 | 10.65 | (Riva et al., 2016) |
| $C_9H_{20}O_4S$ | 223.10095 | 10.71 | (Riva et al., 2016; Meade et al., 2016) |
| $C_{10}H_{22}O_4S$ | 237.11660 | 10.75 | (Huang et al., 2023) |
| $C_{11}H_{22}O_5S$ | 265.11152 | 10.79 | (Yang et al., 2024) |
| $C_{13}H_{26}O_5S$ | 293.14282 | 10.99 | (Yang et al., 2024) |
| $C_{14}H_{28}O_5S$ | 308.16629 | 11.06 | (Yang et al., 2024) |
| **Monoterpene OSs and NOSs** | | | |
| $C_8H_{14}O_7S$ | 253.03875 | 1.00 | (Hettiyadura et al., 2019; Xu et al., 2015) |
| $C_9H_{12}O_7S$ | 263.02310 | 1.03 | (Brüggemann et al., 2019; Xu et al., 2021) |
| $C_9H_{16}O_6S$ | 251.05948 | 1.04 | (Hettiyadura et al., 2019; Xu et al., 2015) |
| $C_9H_{16}O_7S$ | 267.05440 | 1.02 | (Xu et al., 2015; Meade et al., 2016) |
| $C_9H_{16}O_8S$ | 283.04931 | 1.01 | (Brüggemann et al., 2019; Meade et al., 2016) |
| $C_9H_{16}O_9S$ | 299.04423 | 1.00 | (Brüggemann et al., 2019) |
| $C_{10}H_{14}O_9S$ | 309.02858 | 0.99 | (Brüggemann et al., 2019) |
| $C_{10}H_{16}O_5S$ | 247.06457 | 1.01 | (Xu et al., 2015; Ma et al., 2014) |

87 **Table S4** Continued

| | | | |
|---|---|---|---|
| $C_9H_{18}O_7S$ | 269.07005 | 1.03 | (Riva et al., 2016; Brüggemann et al., 2019) |
| $C_{10}H_{16}O_6S$ | 263.05948 | 1.02 | (Ma et al., 2014) |
| $C_{10}H_{16}O_7S$ | 279.05440 | 1.00 | (Ma et al., 2014; Xu et al., 2015; Meade et al., 2016; Hettiyadura et al., 2019) |
| $C_{10}H_{16}O_8S$ | 295.04931 | 1.01 | (Riva et al., 2016; Brüggemann et al., 2019) |
| $C_{10}H_{18}O_5S$ | 249.0806 | 1.02 | (Xu et al., 2015; Ma et al., 2014; Xu et al., 2021; Wang et al., 2017; Hansen et al., 2014) |
| $C_{10}H_{18}O_6S$ | 265.07513 | 1.02 | (Brüggemann et al., 2019; Ma et al., 2014) |
| $C_{10}H_{18}O_7S$ | 281.07005 | 1.01 | (Hettiyadura et al., 2019; Ma et al., 2014) |
| $C_{10}H_{18}O_8S$ | 297.06496 | 1.02 | (Xu et al., 2015; Meade et al., 2016) |
| $C_{10}H_{20}O_5S$ | 251.09587 | 1.03 | (Riva et al., 2016; Brüggemann et al., 2019) |
| $C_{10}H_{20}O_6S$ | 267.09078 | 1.05 | (Brüggemann et al., 2019) |
| $C_{10}H_{20}O_7S$ | 283.08570 | 1.03 | (Brüggemann et al., 2019; Ma et al., 2014) |
| $C_9H_{15}O_8NS$ | 296.04456 | 5.61 | (Hettiyadura et al., 2019; Xu et al., 2015; Xu et al., 2021) |
| $C_{10}H_{17}O_7NS$ | 294.06530 | 9.26 | (Hettiyadura et al., 2019; Meade et al., 2016; Xu et al., 2021; Le Breton et al., 2018) |
| $C_{10}H_{17}O_8NS$ | 310.06021 | 8.27 | (Xu et al., 2015; Ma et al., 2014) |
| $C_{10}H_{17}O_9NS$ | 326.05513 | 8.50 | (Xu et al., 2015; Meade et al., 2016) |
| $C_{10}H_{17}O_{10}NS$ | 342.05004 | 5.01 | (Xu et al., 2015; Meade et al., 2016; Hettiyadura et al., 2019) |
| $C_{10}H_{19}O_8NS$ | 312.07586 | 7.59 | (Stone et al., 2012) |
| $C_{10}H_{19}O_9NS$ | 328.07078 | 5.37 | (Xu et al., 2015) |
| **Sesquiterpene OSs and NOSs** | | | |
| $C_{14}H_{26}O_6S$ | 321.13773 | 10.76 | (Chan et al., 2011) |
| $C_{14}H_{28}O_6S$ | 323.15338 | 10.85 | (Tao et al., 2014) |
| $C_{14}H_{30}O_4S$ | 293.17920 | 11.88 | (Tao et al., 2014) |
| $C_{15}H_{26}O_7S$ | 349.13265 | 8.98 | (Chan et al., 2011) |
| $C_{14}H_{22}O_7S$ | 333.10135 | 9.01 | (Chan et al., 2011) |
| $C_{15}H_{25}O_7NS$ | 362.12790 | 11.55 | (Chan et al., 2011) |

88

89

90 **Table S5** The formula, classification, and $MS^2$ fragments of Unknown OSs and NOSs

| Formula | Classification | *m/z* | $MS^2$ fragments | | | |
|---|---|---|---|---|---|---|
| | | ($[M-H]^-$) | $[C_nH_{2n+1}]^-$ | $[C_nH_{2n-1}]^-$ | $[C_nH_{2n-3}]^-$ | $[C_6H_5R-H]^-$ |
| $C_{12}H_{26}O_4S$ | | 265.14790 | √ | | | |
| $C_{13}H_{28}O_4S$ | | 279.16355 | √ | | | |
| $C_{15}H_{32}O_4S$ | | 307.19485 | √ | | | |
| $C_{16}H_{34}O_4S$ | | 321.21050 | √ | | | |
| $C_{18}H_{38}O_4S$ | | 349.24180 | √ | | | |
| $C_{20}H_{42}O_4S$ | | 377.27310 | √ | | | |
| $C_{22}H_{46}O_4S$ | | 405.30440 | √ | | | |
| $C_{23}H_{46}O_4S$ | | 417.30440 | √ | | | |
| $C_{23}H_{48}O_4S$ | | 419.32005 | √ | | | |
| $C_{24}H_{50}O_4S$ | | 433.33570 | √ | | | |
| $C_{25}H_{52}O_4S$ | | 447.35135 | √ | | | |
| $C_{26}H_{54}O_4S$ | | 461.36700 | √ | | | |
| $C_{12}H_{26}O_5S$ | | 281.14282 | √ | | | |
| $C_{13}H_{28}O_5S$ | | 295.15847 | √ | | | |
| $C_{14}H_{30}O_5S$ | | 309.17412 | √ | | | |
| $C_{16}H_{32}O_5S$ | | 335.18977 | √ | | | |
| $C_{16}H_{34}O_5S$ | | 337.20542 | √ | | | |
| $C_{18}H_{36}O_5S$ | | 363.22107 | √ | | | |
| $C_{19}H_{38}O_5S$ | | 377.23672 | √ | | | |
| $C_{20}H_{40}O_5S$ | | 391.25237 | √ | | | |
| $C_{10}H_{22}O_6S$ | Aliphatic OSs | 269.10643 | √ | | | |
| $C_{11}H_{22}O_6S$ | | 281.10643 | √ | | | |
| $C_{11}H_{24}O_6S$ | | 283.12208 | √ | | | |
| $C_{12}H_{24}O_6S$ | | 295.12208 | √ | | | |
| $C_{16}H_{32}O_6S$ | | 351.18468 | √ | | | |
| $C_{17}H_{34}O_6S$ | | 365.20033 | √ | | | |
| $C_{18}H_{34}O_6S$ | | 377.20033 | √ | | | |
| $C_{18}H_{36}O_6S$ | | 379.21598 | √ | | | |
| $C_{24}H_{44}O_6S$ | | 459.27858 | | | √ | |
| $C_{11}H_{20}O_7S$ | | 295.08570 | | | | |
| $C_{12}H_{20}O_7S$ | | 307.08570 | | √ | | |
| $C_{16}H_{32}O_7S$ | | 367.17960 | √ | | | |
| $C_{18}H_{34}O_7S$ | | 393.19525 | √ | | | |
| $C_{19}H_{38}O_7S$ | | 409.22655 | √ | | | |
| $C_{20}H_{38}O_7S$ | | 421.22655 | √ | | | |
| $C_{21}H_{40}O_7S$ | | 435.24220 | √ | | | |
| $C_{21}H_{42}O_7S$ | | 437.25785 | √ | | | |
| $C_8H_{16}O_8S$ | | 271.04931 | | | | |
| $C_{18}H_{34}O_8S$ | | 409.19016 | √ | | | |
| $C_{19}H_{38}O_8S$ | | 425.22146 | √ | | | |
| $C_{25}H_{48}O_8S$ | | 507.29971 | √ | | | |

91 **Table S5** Continued

| | | | | | | |
|---|---|---|---|---|---|---|
| $C_{10}H_{21}NO_7S$ | | 298.09660 | √ | | | |
| $C_{11}H_{23}NO_7S$ | | 312.11225 | √ | | | |
| $C_{12}H_{25}NO_7S$ | | 326.12790 | √ | | | |
| $C_{13}H_{27}NO_7S$ | | 340.14355 | √ | | | |
| $C_{14}H_{29}NO_7S$ | | 354.15920 | √ | | | |
| $C_{15}H_{31}NO_7S$ | | 368.17485 | √ | | | |
| $C_{16}H_{33}NO_7S$ | | 382.19050 | √ | | | |
| $C_{17}H_{35}NO_7S$ | | 396.20615 | √ | | | |
| $C_{18}H_{37}NO_7S$ | Aliphatic | 410.22180 | √ | | | |
| $C_{19}H_{37}NO_7S$ | NOSs | 422.22180 | | √ | | |
| $C_{19}H_{39}NO_7S$ | | 424.23745 | √ | | | |
| $C_{21}H_{43}NO_7S$ | | 452.26875 | √ | | | |
| $C_8H_{17}NO_8S$ | | 286.06021 | √ | | | |
| $C_9H_{19}NO_8S$ | | 300.07586 | √ | | | |
| $C_{12}H_{25}NO_8S$ | | 342.12281 | √ | | | |
| $C_{19}H_{39}NO_8S$ | | 440.23236 | √ | | | |
| $C_{21}H_{41}NO_8S$ | | 466.24801 | | √ | | |
| $C_{18}H_{35}NO_9S$ | | 440.19598 | | √ | | |
| $C_8H_{12}O_8S$ | | 267.01801 | | | √ | |
| $C_8H_{14}O_8S$ | | 269.03366 | | | | |
| $C_{10}H_{14}O_8S$ | | 293.03366 | | | | |
| $C_8H_{12}O_9S$ | Monoterpene | 283.01293 | | | √ | |
| $C_8H_{14}O_9S$ | OSs | 285.02858 | | | | |
| $C_{10}H_{18}O_9S$ | | 313.05988 | | | | |
| $C_9H_{12}O_{10}S$ | | 311.00784 | | | √ | |
| $C_9H_{14}O_{10}S$ | | 313.02349 | | | | |
| $C_8H_{13}NO_7S$ | | 266.03400 | | | √ | |
| $C_9H_{15}NO_7S$ | | 280.04965 | | | √ | |
| $C_8H_{13}NO_8S$ | Monoterpene | 282.02891 | | | | |
| $C_{10}H_{15}NO_8S$ | NOSs | 308.04456 | | | √ | |
| $C_8H_{13}NO_9S$ | | 298.24255 | | | | |
| $C_{10}H_{19}NO_{10}S$ | | 344.06569 | | | | |
| $C_8H_{13}NO_{11}S$ | | 330.01365 | | | | |
| $C_{10}H_8O_8S$ | | 286.98671 | | | | √ |
| $C_8H_{10}O_8S$ | | 265.00236 | | | | √ |
| $C_8H_{10}O_9S$ | | 280.99728 | | | | √ |
| $C_{10}H_{10}O_8S$ | | 289.00236 | | | | √ |
| $C_{10}H_{12}O_8S$ | Aromatic OSs | 291.01801 | | | | √ |
| $C_{11}H_{12}O_6S$ | | 271.02818 | | | | √ |
| $C_{14}H_{12}O_5S$ | | 291.29755 | | | | √ |
| $C_{16}H_{22}O_8S$ | | 374.10409 | | | | √ |
| $C_{21}H_{30}O_5S$ | | 393.17412 | | | | √ |

92

93 **Table S5** Continued

| | | | |
|---|---|---|---|
| $C_{22}H_{32}O_5S$ | Aromatic OSs | 407.18977 | √ |
| $C_{30}H_{48}O_4S$ | | 503.32005 | √ |
| $C_8H_{11}NO_7S$ | | 265.02617 | √ |
| $C_8H_{11}NO_8S$ | Aromatic | 281.02109 | |
| $C_{10}H_{11}NO_7S$ | NOSs | 288.01835 | √ |
| $C_{16}H_{27}NO_8S$ | | 392.13846 | √ |

94 *: common fragments, including $[HSO_4]^-$ (*m/z* 96.96010) and $[ONO_2]^-$ (*m/z* 61.98837) were not
95 listed in Table S5

96

**Table S6.** The mass concentrations of $PM_{2.5}$ and its chemical composition, gaseous pollutants concentrations, and the mean values of the meteorological parameters.

| Species (unit) | Beijing | Taiyuan | Changsha |
|---|---|---|---|
| $PM_{2.5}$ ($\mu g/m^3$) | 46.65 ± 30.43 | 73.15 ± 49.73 | 66.05 ± 49.20 |
| $NO_3^-$ ($\mu g/m^3$) | 11.96 ± 12.40 | 14.36 ± 9.75 | 34.86 ± 30.02 |
| $SO_4^{2-}$ ($\mu g/m^3$) | 5.34 ± 5.91 | 11.50 ± 9.84 | 9.84 ± 6.00 |
| $NH_4^+$ ($\mu g/m^3$) | 5.66 ± 6.06 | 9.00 ± 6.75 | 10.68 ± 8.04 |
| OC ($\mu g/m^3$) | 4.53 ± 2.40 | 9.05 ± 4.86 | 9.75 ± 5.46 |
| $SO_2$ ($\mu g/m^3$) | 3.10 ± 1.19 | 18.23 ± 8.86 | 6.60 ± 2.07 |
| $NO_2$ ($\mu g/m^3$) | 44.98 ± 19.36 | 62.21 ± 23.85 | 46.60 ± 17.73 |
| CO ($mg/m^3$) | 0.73 ± 0.32 | 1.34 ± 0.59 | 1.08 ± 0.42 |
| $O_3$ ($\mu g/m^3$) | 22.58 ± 15.80 | 24.71 ± 19.69 | 26.12 ± 12.88 |
| OSs ($ng/m^3$) | 41.11 ± 34.47 | 57.39 ± 39.23 | 102.06 ± 80.54 |
| RH (%) | 47.97 ± 19.04 | 50.73 ± 15.62 | 71.45 ± 13.75 |
| Temperature (°C) | 0.62 ± 6.58 | -2.58 ± 4.82 | 7.79 ± 3.52 |

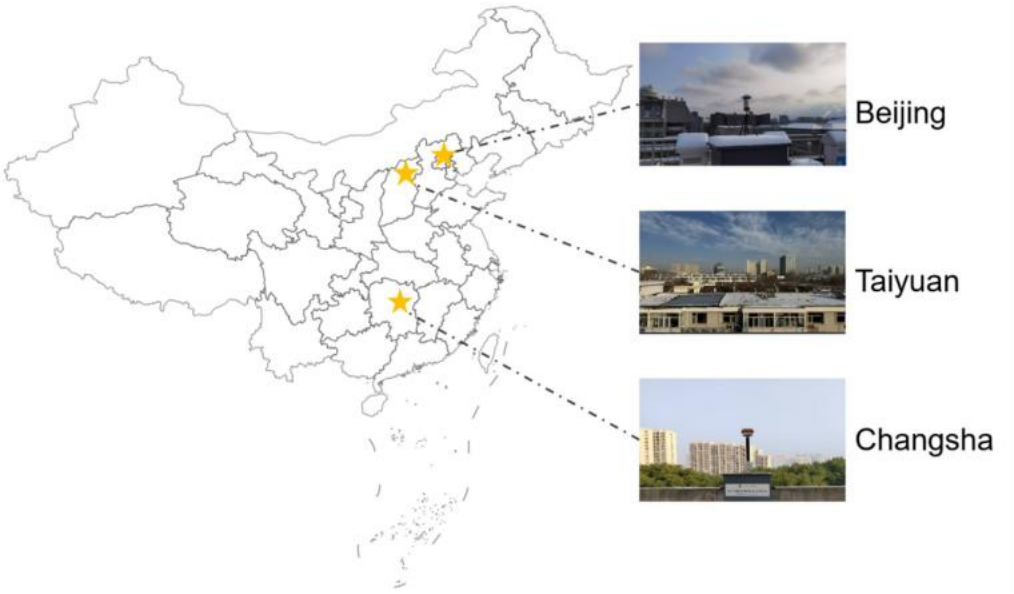


100

101 **Figure S1.** The geographical locations of the sample sites in this study.

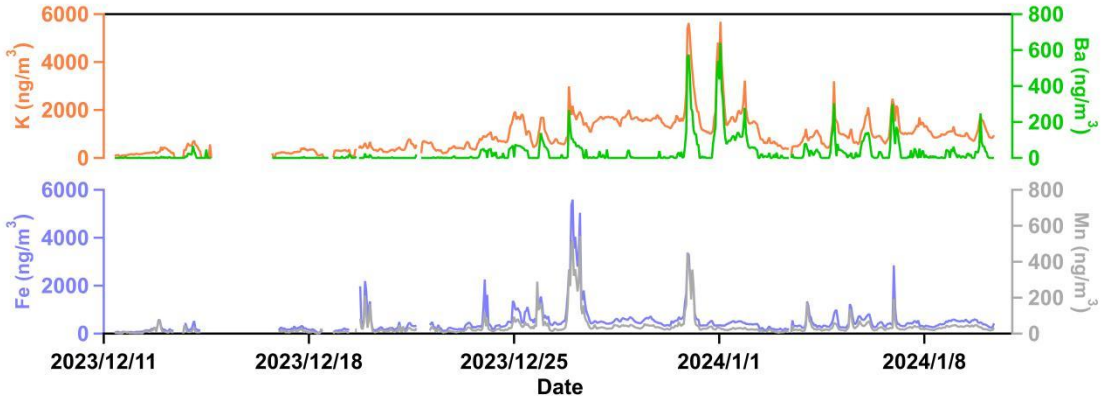


**Figure S2.** Time series of Ba, K, Fe and Mn concentrations in Changsha.

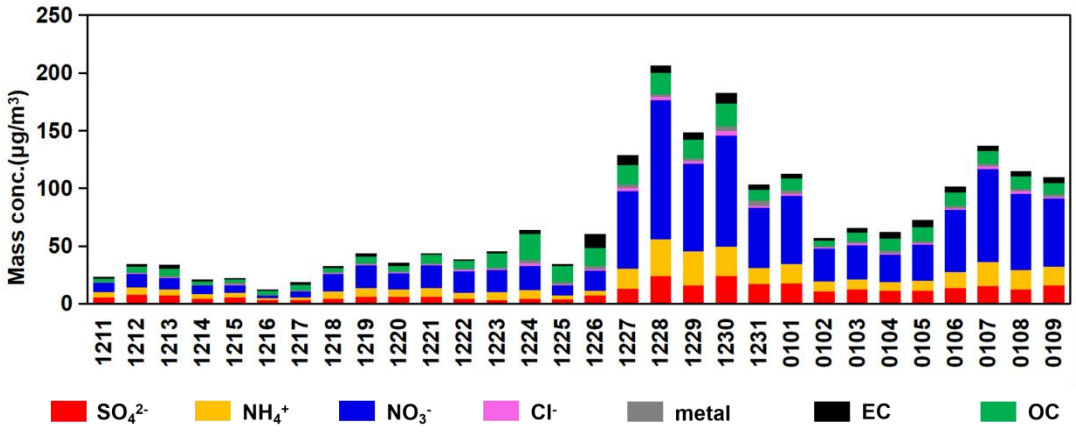


**Figure S3.** Time series of chemical components concentrations in Changsha.

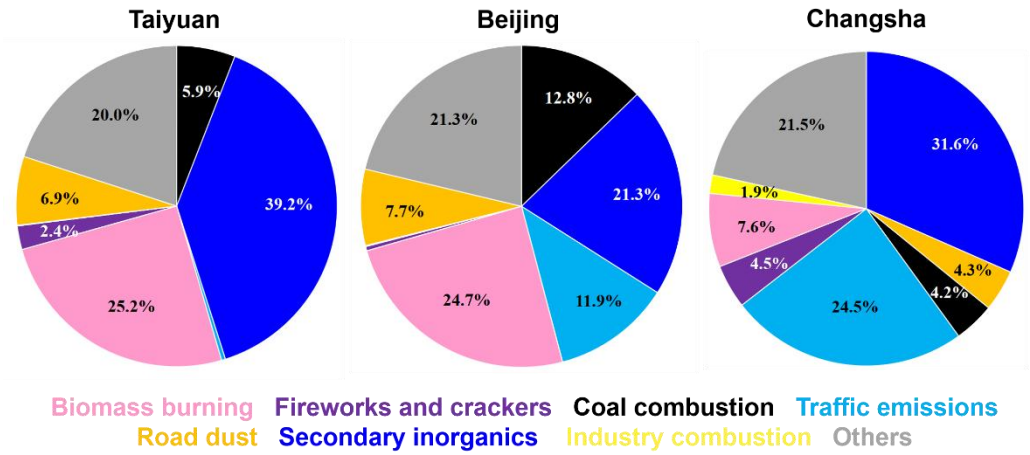


**Figure S4.** Contribution of different sources to $PM_{2.5}$ mass in three sites.

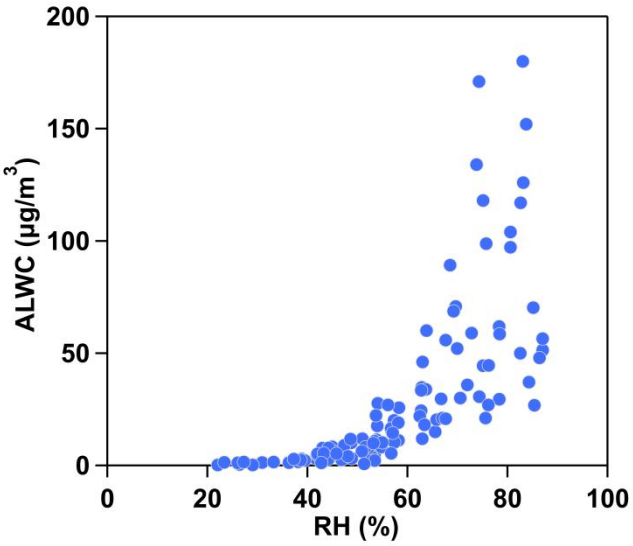


**Figure S5.** Aerosol liquid water content (ALWC) as a function of the relative humidity (RH).

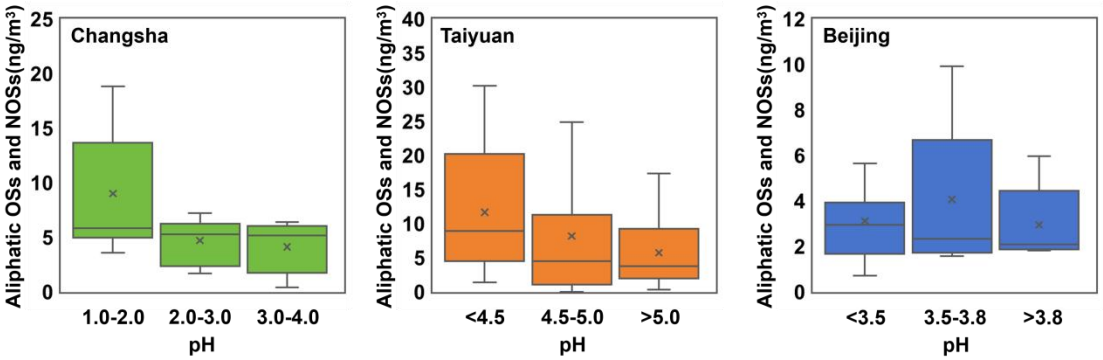


**Figure S6.** The mass concentrations of OSs under different pH levels.

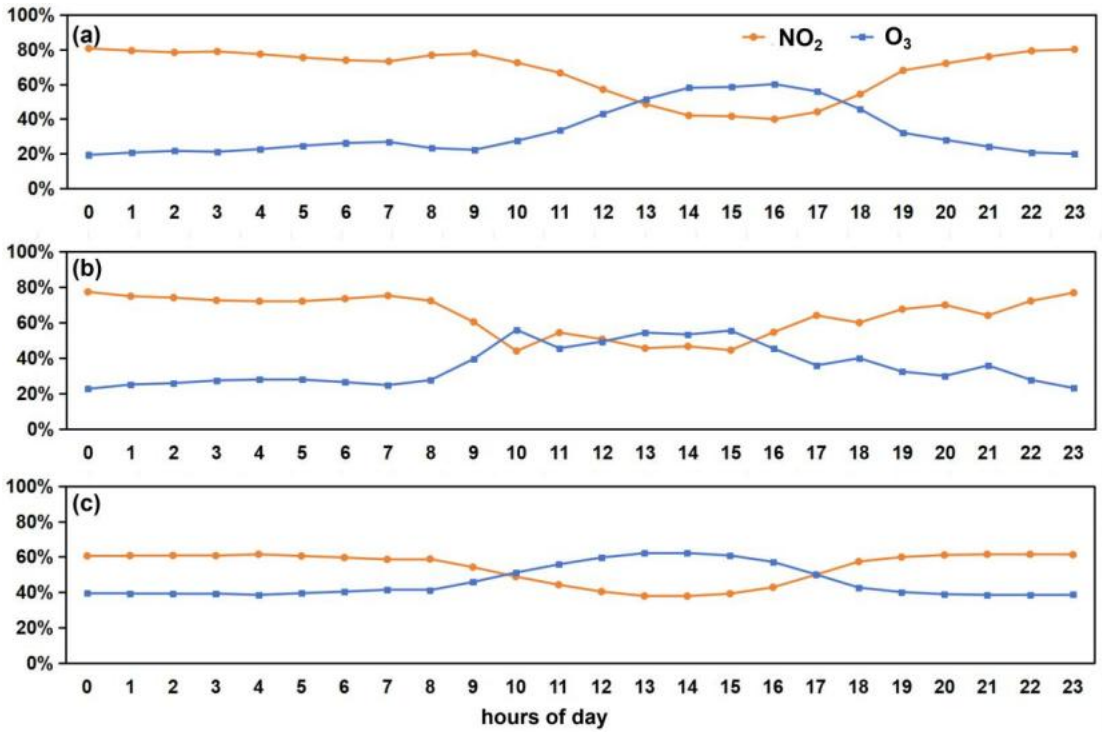


**Figure S7.** Diurnal variations of the distribution of $NO_2$, and $O_3$ on $O_x$ in (a) Changsha, (b) Taiyuan, and (c) Beijing.

## References


Brüggemann, M., van Pinxteren, D., Wang, Y. C., Yu, J. Z., Herrmann, H.: Quantification of known and unknown terpenoid organosulfates in PM10 using untargeted LC-HRMS/MS: contrasting summertime rural Germany and the North China Plain. ENVIRONMENTAL CHEMISTRY. 16, 333-346. 10.1071/EN19089, 2019.

Chan, M. N., Surratt, J. D., Chan, A. W. H., Schilling, K., Offenberg, J. H., Lewandowski, M., Edney, E. O., Kleindienst, T. E., Jaoui, M., Edgerton, E. S., Tanner, R. L., Shaw, S. L., Zheng, M., Knipping, E. M., Seinfeld, J. H.: Influence of aerosol acidity on the chemical composition of secondary organic aerosol from β-caryophyllene. Atmos. Chem. Phys. 11, 1735-1751. 10.5194/acp-11-1735-2011, 2011.

Fountoukis, C., Nenes, A.: ISORROPIA II: a computationally efficient thermodynamic equilibrium model for K+; Ca2+; Mg2+; NH4+; Na+; SO42-; NO3-; Cl-; H2O aerosols. Atmospheric Chemistry and Physics. 7, 4639-4659. 10.5194/acp-7-4639-2007, 2007.

Hansen, A. M. K., Kristensen, K., Nguyen, Q. T., Zare, A., Cozzi, F., Nøjgaard, J. K., Skov, H., Brandt, J., Christensen, J. H., Ström, J., Tunved, P., Krejci, R., Glasius, M.: Organosulfates and organic acids in Arctic aerosols: speciation, annual variation and concentration levels. Atmos. Chem. Phys. 14, 7807-7823. 10.5194/acp-14-7807-2014, 2014.

Hettiyadura, A. P. S., Al-Naiema, I. M., Hughes, D. D., Fang, T., Stone, E. A.: Organosulfates in Atlanta, Georgia: anthropogenic influences on biogenic secondary organic aerosol formation. Atmos. Chem. Phys. 19, 3191-3206. 10.5194/acp-19-3191-2019, 2019.

Huang, L., Wang, Y., Zhao, Y., Hu, H., Yang, Y., Wang, Y., Yu, J.-Z., Chen, T., Cheng, Z., Li, C., Li, Z., Xiao, H.: Biogenic and Anthropogenic Contributions to Atmospheric Organosulfates in a Typical Megacity in Eastern China. 128, e2023JD038848. https://doi.org/10.1029/2023JD038848, 2023.

Le Breton, M., Wang, Y., Hallquist, Å. M., Pathak, R. K., Zheng, J., Yang, Y., Shang, D., Glasius, M., Bannan, T. J., Liu, Q., Chan, C. K., Percival, C. J., Zhu, W., Lou, S., Topping, D., Wang, Y., Yu, J., Lu, K., Guo, S., Hu, M., Hallquist, M.: Online gas- and particle-phase measurements of organosulfates, organosulfonates and nitrooxy organosulfates in Beijing utilizing a FIGAERO ToF-CIMS. Atmos. Chem. Phys. 18, 10355-10371. 10.5194/acp-18-10355-2018, 2018.

Ma, Y., Xu, X., Song, W., Geng, F., Wang, L.: Seasonal and diurnal variations of particulate organosulfates in urban Shanghai, China. Atmospheric Environment. 85, 152-160. https://doi.org/10.1016/j.atmosenv.2013.12.017, 2014.

Meade, L. E., Riva, M., Blomberg, M. Z., Brock, A. K., Qualters, E. M., Siejack, R. A., Ramakrishnan, K., Surratt, J. D., Kautzman, K. E.: Seasonal variations of fine particulate organosulfates derived from biogenic and anthropogenic hydrocarbons in the mid-Atlantic United States. Atmospheric Environment. 145, 405-414. https://doi.org/10.1016/j.atmosenv.2016.09.028, 2016.

Riva, M., Tomaz, S., Cui, T., Lin, Y.-H., Perraudin, E., Gold, A., Stone, E. A., Villenave, E., Surratt, J. D.: Evidence for an Unrecognized Secondary Anthropogenic Source of Organosulfates and Sulfonates: Gas-Phase Oxidation of Polycyclic Aromatic Hydrocarbons in the Presence of Sulfate Aerosol. Environmental Science & Technology. 49, 6654-6664. 10.1021/acs.est.5b00836, 2015.

Riva, M., Da Silva Barbosa, T., Lin, Y. H., Stone, E. A., Gold, A., Surratt, J. D.: Chemical characterization of organosulfates in secondary organic aerosol derived from the photooxidation of alkanes. Atmospheric Chemistry and Physics. 16, 11001-11018. 10.5194/acp-16-11001-2016, 2016.

Stone, E. A., Yang, L., Yu, L. E., Rupakheti, M.: Characterization of organosulfates in atmospheric

aerosols at Four Asian locations. Atmospheric Environment. 47, 323-329. https://doi.org/10.1016/j.atmosenv.2011.10.058, 2012.

Tao, S., Lu, X., Levac, N., Bateman, A. P., Nguyen, T. B., Bones, D. L., Nizkorodov, S. A., Laskin, J., Laskin, A., Yang, X.: Molecular Characterization of Organosulfates in Organic Aerosols from Shanghai and Los Angeles Urban Areas by Nanospray-Desorption Electrospray Ionization High-Resolution Mass Spectrometry. Environmental Science & Technology. 48, 10993-11001. 10.1021/es5024674, 2014.

Wang, Y., Ren, J., Huang, X. H. H., Tong, R., Yu, J. Z.: Synthesis of Four Monoterpene-Derived Organosulfates and Their Quantification in Atmospheric Aerosol Samples. Environmental Science & Technology. 51, 6791-6801. 10.1021/acs.est.7b01179, 2017.

Xu, L., Guo, H., Boyd, C. M., Klein, M., Bougiatioti, A., Cerully, K. M., Hite, J. R., Isaacman-VanWertz, G., Kreisberg, N. M., Knote, C., Olson, K., Koss, A., Goldstein, A. H., Hering, S. V., de Gouw, J., Baumann, K., Lee, S.-H., Nenes, A., Weber, R. J., Ng, N. L.: Effects of anthropogenic emissions on aerosol formation from isoprene and monoterpenes in the southeastern United States. 112, 37-42. doi:10.1073/pnas.1417609112, 2015.

Xu, L., Yang, Z., Tsona, N. T., Wang, X., George, C., Du, L.: Anthropogenic–Biogenic Interactions at Night: Enhanced Formation of Secondary Aerosols and Particulate Nitrogen- and Sulfur-Containing Organics from β-Pinene Oxidation. Environmental Science & Technology. 55, 7794-7807. 10.1021/acs.est.0c07879, 2021.

Yang, T., Xu, Y., Ma, Y.-J., Wang, Y.-C., Yu, J. Z., Sun, Q.-B., Xiao, H.-W., Xiao, H.-Y., Liu, C.-Q.: Field Evidence for Constraints of Nearly Dry and Weakly Acidic Aerosol Conditions on the Formation of Organosulfates. Environmental Science & Technology Letters. 11, 981-987. 10.1021/acs.estlett.4c00522, 2024.

Yang, Z., Tsona, N. T., Li, J., Wang, S., Xu, L., You, B., Du, L.: Effects of NOx and SO2 on the secondary organic aerosol formation from the photooxidation of 1,3,5-trimethylbenzene: A new source of organosulfates. Environmental Pollution. 264, 114742. https://doi.org/10.1016/j.envpol.2020.114742, 2020.